Journal of Alloys and Compounds 509 (2011) 8917–8921

Contents lists available at ScienceDirect

Journal of Alloys and Compounds

journal homepage: www.elsevier.com/locate/jallcom

Influences of different prior heat treatments on the microstructural and mechanical properties of Cu–Fe filamentary composites

Z.W. Wu[a,*], L. Meng[b]

[a] Airport College, Civil Aviation University of China, Tianjin 300300, China
[b] Department of Materials Science and Engineering, Zhejiang University, Hangzhou 310027, China

ARTICLE INFO

Article history:
Received 26 April 2011
Received in revised form 3 June 2011
Accepted 7 June 2011
Available online 17 June 2011

Keywords:
Metals and alloys
Interface
Mechanical properties
Microstructure

ABSTRACT

Cu–6 wt.% Fe and Cu–12 wt.% Fe filamentary composites were prepared by casting and cold drawing. And a different heat treatment of quenching and aging or homogenizing was introduced before cold drawing process, respectively. The microstructure was observed and the tensile strength measured for the composites at different drawing strains. The quenching and aging or homogenizing prior to drawing deformation refine the as-cast microstructure and result in the increase in interface density in the drawn microstructure. The drawn alloys with the homogenizing treatment show smaller filament spacing than those with the quenching and aging treatment because homogenizing results in smaller and more dispersive primary Fe dendrites before drawing deformation. The heat treatments can improve the strength of the composites by increasing precipitation strengthening and interface strengthening levels. With the reduction in filament spacing during drawing deformation, the strength of the alloys with smaller initial size of Fe dendrites increases more obviously.

1. Introduction

Cu–Fe filamentary composites are the promising candidates of conductor materials in electrical devices due to their high service performance and relatively low cost [1–4]. The filamentary microstructure can generally be produced from the primary as-cast structure of double-phase Cu-based alloys by heavy cold deformation [5–8]. Some investigations indicated that the tensile strength could directly be related to the filament spacing of the drawn microstructure while the filament spacing at a certain drawing strain depended strongly on the dendrite spacing in the as-cast structure [1,9–14]. Therefore, the initial microstructure before drawing deformation can play an important role in the strengthening of Cu–Fe composites. For example, adding Ag into Cu–Fe composites improved the tensile strength because refined primary Fe dendrites and additional Ag filaments reduced the filament spacing [15].

Prior heat treatments before drawing deformation can significantly influence the initial microstructure of the as-cast alloys and therefore modify the filamentary distribution or density of the final drawn structure. Some investigations proved that prior heat treatments had positive effects on the mechanical properties of Cu-based composites. Gaganov et al. [16] indicated that a prior homogenizing heat treatment combined with a subsequent aging before deformation improved the mechanical properties of Cu–7 wt.% Ag and Cu–24 wt.% Ag because discontinuous precipitation reaction was suppressed due to the absence of high-angle grain boundaries or the complete enclosure of Cu dendrites by eutectic colonies in the heat treatment process. Lin and Meng [17] presented the dependence of the hardness on a prior solution and aging treatment, and the relationship between the precipitation behavior and hardening benefit for as-cast Cu–(6–24) wt.% Ag. However, the mentioned investigations in prior heat treatments are only focused on Cu–Ag alloys, which belong to the FCC–FCC matched system of double phases. It can be deduced that an appropriate heat treatment prior to the drawing deformation for Cu–Fe alloys, which belong to the FCC–BCC matched system of double phases, should also change the distribution of initial phases in the as-cast structure and affect the mechanical properties of the deformed structure. Our previous investigations indicated [18] that a prior homogenizing treatment followed by furnace cooling increased the strength of Cu–6 wt.% Fe and Cu–12 wt.% Fe because the precipitation of secondary Fe particles and the dispersion of the primary Fe dendrites were promoted. In this study, Cu–6 wt.% Fe and Cu–12 wt.% Fe filamentary composites were prepared by casting, various prior heat-treating and cold drawing at different strain levels. The microstructure evolution was observed and the ultimate tensile strength determined in order to investigate the influence of different prior heat treatments. The relationship between the microstructure and strength was discussed for the alloys with different prior heat treatments.

* Corresponding author. Tel.: +86 22 24092475; fax: +86 22 24092474.
E-mail address: zwwu@cauc.edu.cn (Z.W. Wu).

0925-8388/$ – see front matter.
doi:10.1016/j.jallcom.2011.06.030

2. Experimental procedure

Electrolytic copper and commercial pure iron were used as starting materials. Cu–6 wt.% Fe (denoted as Cu6Fe) and Cu–12 wt.% Fe (denoted as Cu12Fe) were molten in a vacuum induction furnace and cast into cylindrical ingots in a copper mold. Some of the ingots were solid-solution treated at 1000 °C for 1 h, quenched in water and then aged at 550 °C for 4 h (denoted as PHTI). Other ingots were homogenized at 950 °C for 3 h followed by furnace cooling (denoted as PHTII). The ingots were drawn into wires at ambient temperature. Drawing reduction was described in terms of the logarithmic strain by $\eta = \ln(A_0/A)$ and referred as the draw ratio, where A_0 and A were the original and final cross-sectional areas of the drawn specimens, respectively.

The microstructure was observed by optical microscopy, scanning electron microscopy (SEM) and transmission electron microscopy (TEM). The SEM specimens were prepared by etching the metallographic samples in a solution of 80 ml H_2O, 10 g $K_2Cr_2O_7$ and 5 ml H_2SO_4. The TEM specimens were prepared by mechanically thinning and then ion milling at 5 kV with an incidence angle of 12°. Filament spacing was determined using the geometric-intercept method through the longitudinal image from the SEM images in metallographic examination. Tensile test was conducted at the strain rate of $2.0 \times 10^{-3}\,s^{-1}$ and ambient temperature using the wire specimens of 85.0 mm in gauge length. Each value of the tensile strength was taken from the arithmetical mean measured from three wire specimens.

3. Results

3.1. Microstructure

Optical microstructures for the tested alloys after PHTI are shown in Fig. 1, which compares with the as-cast and tested alloys after PHTII as shown in Fig. 1 in Ref. [18]. In as-cast Cu6Fe and Cu12Fe, some primary Fe dendrites distribute in the Cu matrix and there is a certain extent of solute segregation along boundaries of primary Cu grains. The primary Fe phase in Cu12Fe has higher volume fraction and more developed dendrites than in Cu6Fe due to higher Fe concentration. After prior heat treatments of PHTI and PHTII, the dendrites become finer and more dispersive. Both the alloys after PHTII show smaller scale and more dispersive distribution of the primary Fe dendrites than those after PHTI.

SEM images of Cu12Fe with different prior heat treatments are shown in Fig. 2. TEM images of the secondary particles are also inset in the picture. The primary Fe dendrites can be observed more distinctly to be separated into spheric grains by the prior heat treatments of PHTI and PHTII. Some secondary Fe particles were presented in the alloy during freezing and heat-treating. Small amount of granular and separated Fe particles formed during the freezing process. Fine and dispersive Fe particles precipitated in the

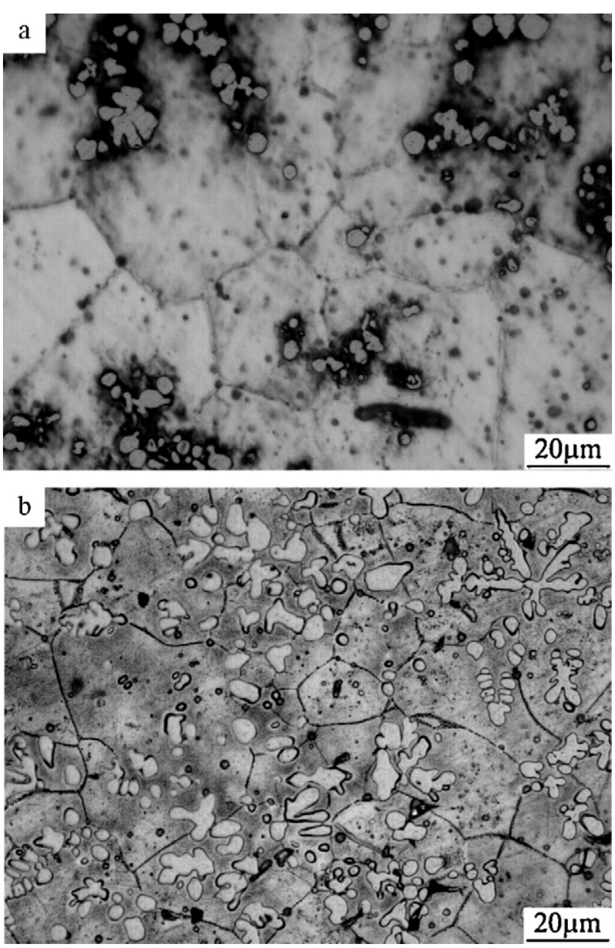

Fig. 1. Optical microstructures of PHTI for (a) Cu6Fe and (b) Cu12Fe.

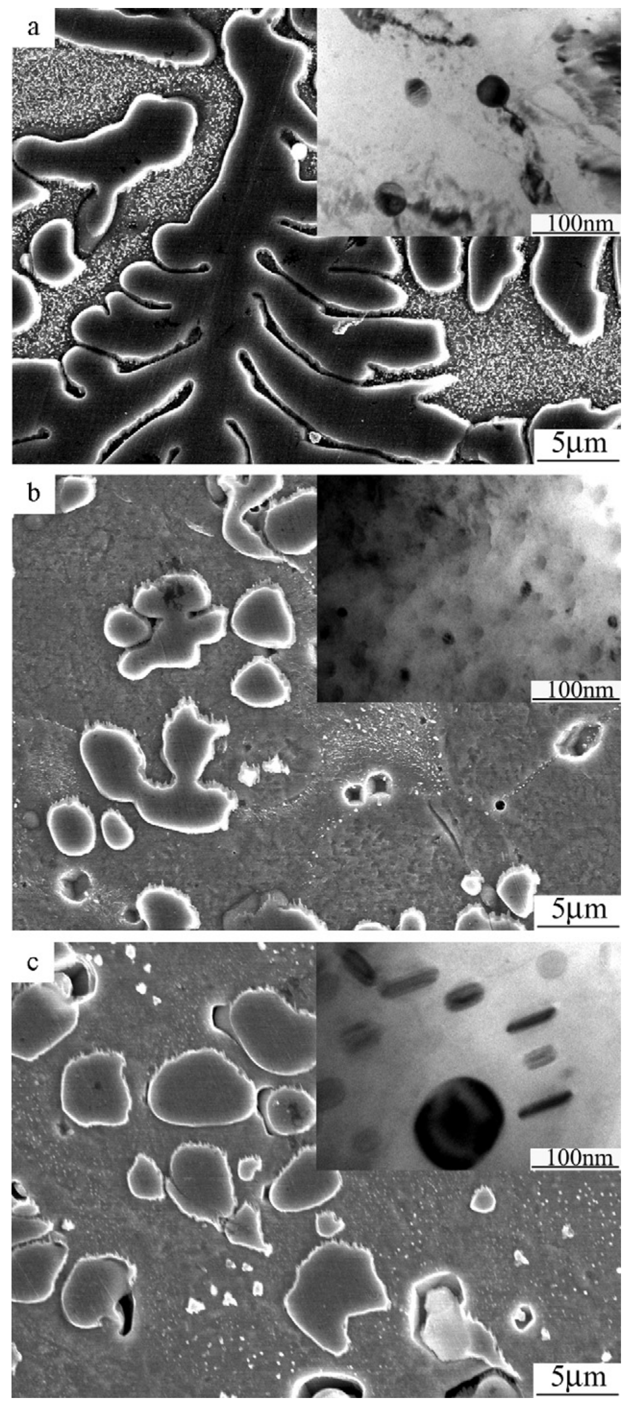

Fig. 2. SEM and inserted TEM images of (a) as-cast, (b) PHTI and (c) PHTII for Cu12Fe.

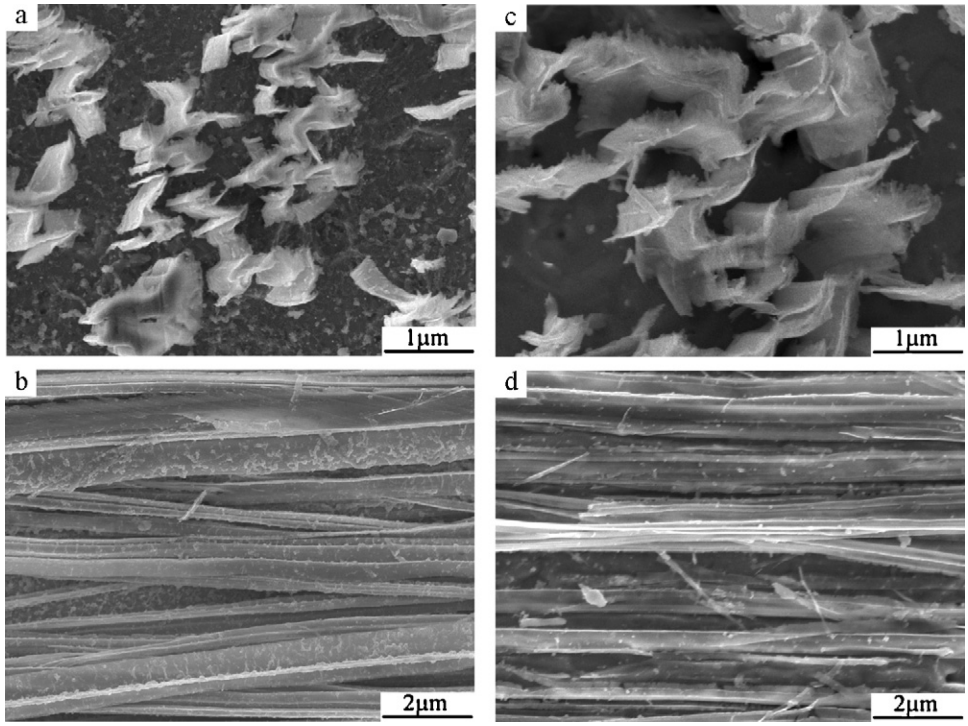

Fig. 3. SEM microstructures of Cu6Fe drawn to $\eta = 7.0$ and treated with (a) PHTI on transverse and (b) longitudinal section, and (c) PHTII on transverse and (d) longitudinal section.

Cu matrix in the alloy with PHTI. Coarse and short-plate Fe particles appeared dispersively in the alloy with PHTII. In general, the secondary Fe particles with the average size of about 0.1–0.3 μm in the alloy with PHTII were larger than that of about 0.01–0.05 μm in the alloy with PHTI.

SEM microstructures of the drawn alloys are shown in Figs. 3 and 4. On the longitudinal section, the original grains and dendrites of both Cu and Fe evolved into ribbon-like filaments during drawing deformation. On the transverse section, the Fe phase shows a curled and folded morphology. The Fe filaments in Cu12Fe

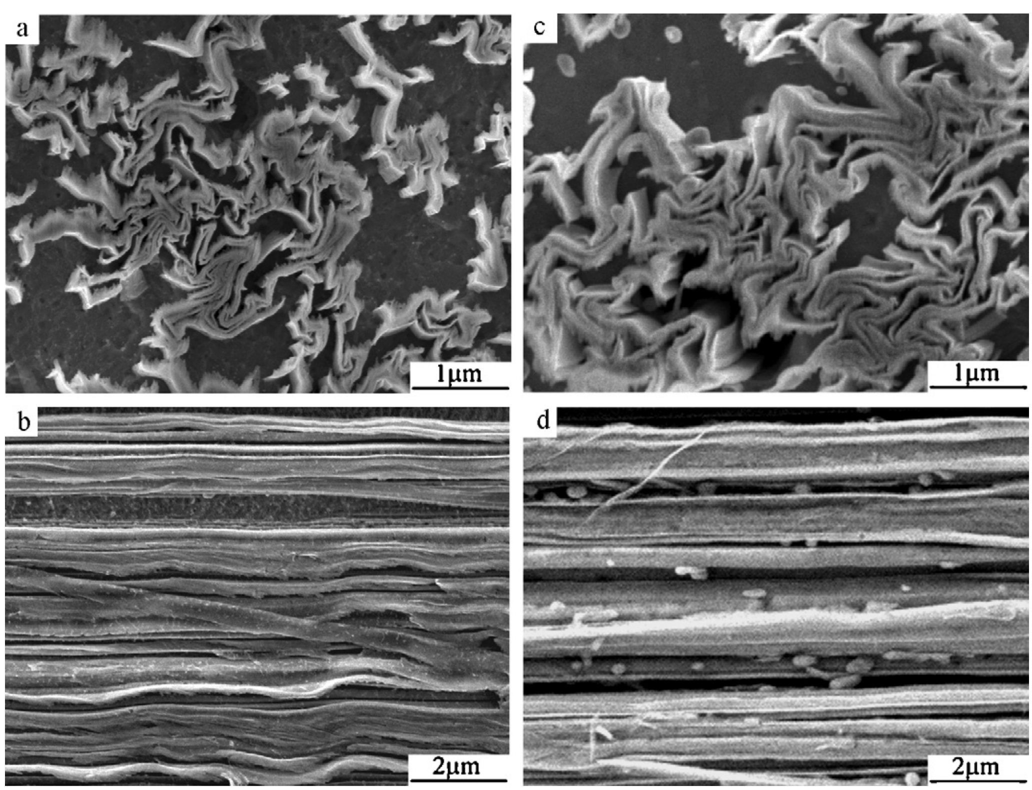

Fig. 4. SEM microstructures of Cu12Fe drawn to $\eta = 7.0$ and treated with (a) PHTI on transverse and (b) longitudinal section, and (c) PHTII on transverse and (d) longitudinal section.

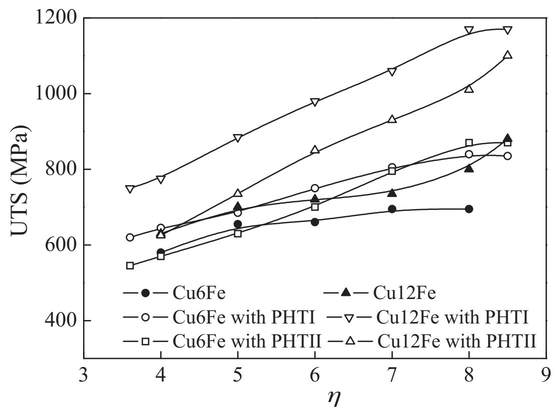

Fig. 5. Ultimate tensile strength dependent on the draw ratio for Cu6Fe and Cu12Fe.

are more compact and finer than in Cu6Fe since Cu12Fe has higher volume fraction of primary Fe and more developed dendrites. As a result of smaller and more dispersive Fe dendrites, the alloys treated with PHTII display a more homogeneous distribution of the filamentary structure than those treated with PHTI at the same drawing deformation.

3.2. Strength

The ultimate tensile strength dependent on the draw ratio is given in Fig. 5. The strength increases with the increasing of draw ratio for all tested composites. Cu12Fe has higher strength than Cu6Fe under the same condition and deformation degree due to higher Fe filament proportion. Both the composites with prior heat treatments show the strength much higher than those without prior heat treatments due to the increase in volume fraction of Fe filaments from the secondary precipitates produced by aging or homogenizing treatment. The quenching and aging treatment seems to induce more significant strengthening than the homogenizing treatment for the alloys under general drawing strain. For example, Cu6Fe at $\eta < 7.0$ and Cu12Fe at all draw ratios with PHTI show the strength higher than both the alloys with PHTII.

4. Discussions

4.1. Microstructure

The formation reason of the primary morphology of as-cast Cu6Fe and Cu12Fe was explained in Ref. [4]. After solid-solution treatment, the dendritic segregation disappeared to a certain degree. The volume fraction of Fe dendrites also decreased because the non-equilibrium products were dissolved into the Cu matrix. The supersaturation level of Fe solute in Cu matrix after solid-solution treatment should generally be higher than that before solid-solution treatment. A more sufficient dynamic condition of precipitation reaction promoted the formation of Fe precipitates in the Cu matrix in aging process. In addition, during homogenization at 950 °C and subsequent furnace cooling, dendritic segregation removed and secondary Fe particles precipitated in the Cu matrix. It is possible that the secondary Cu particles also precipitate in supersaturated primary Fe dendrites and the eutectoid reaction, γ-Fe → Cu + α-Fe, at 850 °C occurs more sufficiently during slow furnace cooling after homogenizing treatment. The formation of secondary and eutectoid Cu particles disperses or separates the Fe dendrites.

The effect of the draw ratio on the Fe filament spacing is shown in Fig. 6. The filament spacing decreases with the increase in draw ratio for the composites with PHTI and PHTII. High volume fraction of Fe dendrites in Cu12Fe than in Cu6Fe must produce small filament spacing during drawing deformation. Moreover, the composites with PHTII have slightly smaller filament spacing than those with PHTI at the same deformation due to the smaller scale and more dispersive distribution of the primary Fe dendrites in the alloys with PHTII before cold drawing. It must be pointed out that the Fe filament spacing is only determined by SEM observation of the filaments evolved from the Fe dendrites. The secondary Fe precipitates also evolved into the Fe filaments during drawing deformation but they were too fine to be distinguished or determined by SEM observation.

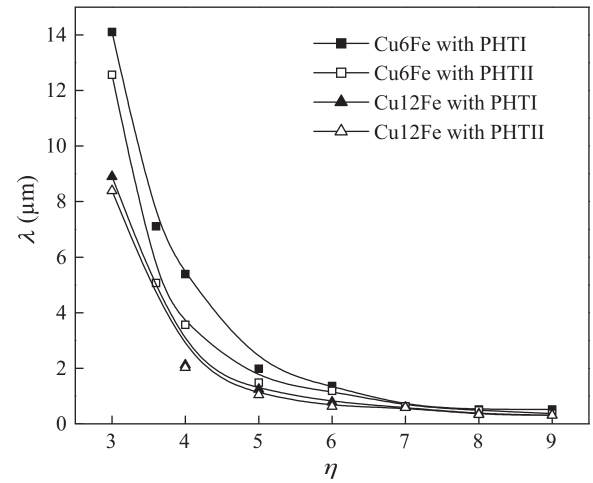

Fig. 6. Fe filament spacing dependent on the draw ratio for Cu6Fe and Cu12Fe.

4.2. Strength

The strengthening mechanism of dislocation multiplication and interface obstacle for Cu-based composites can be considered to be responsible for the behavior of strength change with the draw ratio for the tested alloys [19–21]. In the initial drawing deformation, the increase in dislocation density in filaments with the increase in draw ratio enhances the strength. In the heavy drawing deformation, the strengthening mechanism can be transformed from dislocation multiplication to interface obstacle once the filamentary diameter or filament spacing has approached to a certain scale and the dislocation subcells have tended to disappear [11,20,21]. The interface density of Cu and Fe filaments increases with the decrease in filamentary scale. Moreover, the Fe curling behavior in radial deformation also increases the interface density. The increased interface offers additional resistance to the strain of filamentary structure. Therefore, the strength still increases with the increase in draw ratio for all tested composites in the range of high drawing ratios.

The hardening level of binary Cu-based composites can be expressed by Hall–Petch equation [22]

$$\sigma = \sigma_0 + k\lambda^{-1/2} \quad (1)$$

where σ is the ultimate tensile strength, σ_0 the intrinsic friction stress, k the Hall–Petch coefficient and λ the spacing between filaments. The relationship between the tensile strength and $\lambda^{-1/2}$ is shown in Fig. 7. It is obvious that the experimental results accord well with the Hall–Petch equation or it is certain that there is a linear relationship between the tensile strength and $\lambda^{-1/2}$ for Cu6Fe and Cu12Fe with PHTI and PHTII. Moreover, there is a higher rate of the linear slope for the alloy with smaller initial size of Fe dendrites. For example, the increase rate of the strength dependent on $\lambda^{-1/2}$ is higher for Cu12Fe than for Cu6Fe. Similarly, the increase rate of

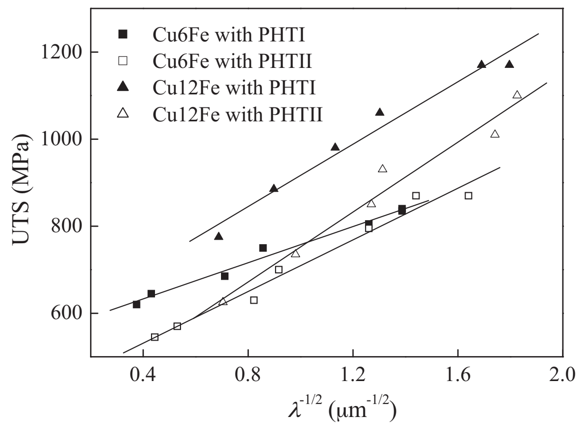

Fig. 7. Ultimate tensile strength dependent on the normalized filament spacing ($\lambda^{-1/2}$) for Cu6Fe and Cu12Fe.

the strength dependent on $\lambda^{-1/2}$ is also higher for the alloys with PHTII than for those with PHTI.

Fine and sufficient Fe precipitates from the quenching and aging treatment prior to drawing deformation in the Cu matrix results in higher strengthening effect in the alloys with PHTI than with PHTII in the initial drawing deformation. Namely, it can be considered that the composites with PHTI should have higher σ_0 than those with PHTII. During subsequent deformation process, coarser Fe precipitates and more separated Fe dendrites in the alloys treated by PHTII than by PHTI can produce later transformation of strengthening mechanism from dislocation multiplication into interface obstacle. The later transformation of strengthening mechanism can keep dislocation subcells to higher draw ratios. Moreover, the alloys treated by PHTII have more uniform distribution of the filamentary structure developed from primary Fe dendrites than those treated by PHTI. The more uniform filamentary structure can result in more reasonable interface distribution in the composites. Therefore, the increase in strength with the decrease in filament spacing is more significant in the composites with PHTII than with PHTI at higher drawing strains.

5. Conclusions

The microstructure of as-cast Cu–6 wt.% Fe and Cu–12 wt.% Fe is composed of primary dendritic grains of Fe and Cu. Quenching and aging treatment or homogenizing treatment prior to drawing deformation removes the solute segregation along Cu grain boundaries, separates the primary dendrites and promotes the precipitation of secondary Fe particles.

The primary Cu and Fe dendrites and secondary Fe particles evolve into the composite filamentary structure during drawing deformation. Heat treatments prior to drawing deformation result in more uniform distribution and smaller scale of the composite filaments formed in subsequent heavy drawing. The filament spacing in the homogenized alloys is smaller than that in the quenched and aged alloys at the same draw ratios because homogenizing treatment produces finer and more uniform primary Fe dendrites.

Heat treatments, in particular, quenching and aging, prior to drawing deformation improve the strength levels of the composite filamentary structure. The strength of the alloy with smaller initial size of Fe dendrites increases more obviously with the reduction in filament spacing. The increase in precipitation strengthening and interface strengthening from prior heat treatments can be responsible for the strength improvement.

References

[1] C. Biselli, D.G. Morris, Acta Mater. 44 (1996) 493–504.
[2] S.I. Hong, P.H. Kim, Y.C. Choi, Scripta Mater. 51 (2004) 95–99.
[3] S.I. Hong, J.S. Song, H.S. Kim, Scripta Mater. 45 (2001) 1295–1300.
[4] Z.W. Wu, J. Alloys Compd. 467 (2009) 213–218.
[5] X. Sauvage, R. Pippan, Mater. Sci. Eng. A 410–411 (2005) 345–347.
[6] L. Zhang, L. Meng, Scripta Mater. 52 (2005) 1187–1191.
[7] X. Sauvage, F. Wetscher, P. Pareige, Acta Mater. 53 (2005) 2127–2135.
[8] Y.L. Wang, K. Han, Y. Huang, K.Y. Zhang, Mater. Sci. Eng. A 351 (2003) 214–223.
[9] J.S. Song, S.I. Hong, H.S. Kim, J. Mater. Process. Technol. 113 (2001) 310–616.
[10] Y.S. Go, W.A. Spitzig, J. Mater. Sci. 26 (1991) 163–171.
[11] G.A. Jerman, I.E. Anderson, J.D. Verhoeven, Metall. Mater. Trans. A 24A (1993) 35–42.
[12] E. Botcharova, J. Freudenberger, A. Gaganov, K. Khlopkov, L. Schultz, Mater. Sci. Eng. A 416 (2006) 261–268.
[13] A. Shikov, V. Pantsyrnyi, A. Vorobieva, N. Khlebova, A. Silaev, Physica C 354 (2001) 410–414.
[14] Z.W. Wu, Y. Chen, L. Meng, J. Alloys Compd. 477 (2009) 198–204.
[15] B.D. Sun, H.Y. Gao, J. Wang, D. Shu, Mater. Lett. 61 (2007) 1002–1006.
[16] A. Gaganov, J. Freudenberger, W. Grünberger, L. Schultz, Z. Metallkd. 95 (2004) 425–432.
[17] J. Lin, L. Meng, J. Alloys Compd. 454 (2008) 150–155.
[18] Z.W. Wu, Y. Chen, L. Meng, J. Alloys Compd. 481 (2009) 236–240.
[19] L. Zhang, L. Meng, J.B. Liu, Scripta Mater. 52 (2005) 587–592.
[20] S.I. Hong, M.A. Hill, Acta Mater. 46 (1998) 4111–4122.
[21] A. Benghalem, D.G. Morris, Acta Mater. 45 (1997) 397–406.
[22] J.S. Song, J.H. Ahn, H.S. Kim, S.I. Hong, J. Mater. Sci. 36 (2001) 5881–5884.